

Application of machine learning algorithms to predict mechanical properties of aluminum alloys

Oleksii Popov¹

¹ Zaporizhzhia National University, Zaporizhzhia, Ukraine

*Corresponding author E-mail: arahorn90@gmail.com

ABSTRACT

Alloys used in aerospace, automotive industries and structural engineering have good strength to specific weight ratio, corrosion resistance and workability. Mechanical properties like tensile and yield strengths, elongation and hardness are vital to ensure integrity of structures. However, conventional techniques in measuring these properties are time consuming, tedious and destructive. This paper provides a framework in which limited experimental data & Machine Learning algorithms are employed to evaluate the important mechanical properties of aerospace grade aluminum alloys. Data set of alloy compositions as well as processing parameters were obtained through material libraries to train and validate through techniques like Random Forest Regression (RFR), Artificial Neural Networks (ANN) and Support Vector Regression. The tensile strength was predicted with the best results for R – Squared & Root Mean Squared Errors were Coefficient of Determination $R^2= 0.96$, RMSE = 12.4 MPa using ANN and RFR were more efficient in predicting the elongation ($R^2>0.93$). The given approach demonstrated a better performance than the ordinary regression approaches with over 20 percent improvement and less experimental work up to about 60%. This approach provides a boosted & scalable approach to greatly increase the pace of material design and mechanical characterization of applications in the aerospace industry.

Keywords: Alloys, Machine Learning, Mechanical Properties of Materials, Aerospace, Aluminum

1. Introduction

The use of aluminum alloys is core to present day application in the engineering field especially in the aerospace industry, the automobile industry and in construction. They have high strength-to-weight ratio, very corrosion resistant, thermally conductive and formable, making them ideal in light-weight structural elements and complicated load bearing structures [1]. Aerospace-grade aluminum alloys have been important in many of its applications, especially because of the demand of mechanical requirements in aircraft and space vehicle structures. Things like tensile strength, yield strength, hardness, and elongation are the most important mechanical properties in such spheres [2]. The properties determine the suitability of a material in particular design functions, limits of safety and durability of service performance in the long run [3].

In the traditional context, the mechanical property testing is based on standardized experimental methods related to tensile testing, hardening test, and even fatigue [4]. Although these techniques are necessary in the formation of the baseline performance records, most of them are time-consuming, labor-intensive, and destructive in nature. Additionally, such testing procedures are also very time and resource consuming in research and manufacturing facilities where a quick screening of new alloy compositions or heat treatment sequences must be carried out [5]. Moreover, these techniques require expensive equipment, specific conditions, and give insufficient measurement accuracy.

The current development of Machine Learning (ML) proposed various prospects of alternatives towards materials properties prediction, especially in the computational materials science location. ML models can calculate the non-linear, complicated relations between the composition of the material being processed, processing conditions and the measured property of the material [6]. The applicability of ML models in the prediction of mechanical, thermal and corrosion behavior of different metallic systems was determined in IN

recent studies [7], [8], [9], [10], [11], [12], [13], [14]. Nevertheless, although the number of research is increasing, the problem of how to choose and confirm the most suitable ML algorithms to predict the mechanical characteristics of aluminum alloys is by now not solved completely. The scope of mechanical properties studied in most previous works has been limited as regards to predictive models of different grades of alloys.

With the aim of filling this gap, the proposed research focuses on combining a curated experimental data with the multiple machine learning approaches to accurately predict the mechanical properties of the aerospace-grade aluminum alloys using their chemical compositions. This task is concerned to compare the performance of various algorithms, which are Random Forest, the Support Vector Regression, and Artificial Neural Networks so that in terms of reliability and comprehensibility the best model could be applied in practice [15-17]. In addition to that, the paper checks the potential of validation of experimental data with machine learning to mitigate the cost of destructive testing of alloy design and speed up the alloy design process. Ultrasonic testing (UT), X-ray testing and eddy current testing are examples of non-destructive testing methods which allow subjecting various mechanical properties of the material, including tensile strength, hardness and ductility, to evaluation, without damaging the material. Such techniques are fast, cost-efficient and can ensure that surface and subsurface defects are detected, which affects the performance of material. NDT is essential in speeding up material design and quality control especially in the case of critical alloys utilized and adapted in industries such as the aerospace industries [18], [19].

ML has found its way as one of the transformative tools in materials science where it has given researchers the power to predict material properties at an even higher accuracy and efficiency rate. Conventional techniques of measuring mechanical properties like tensile strength, Hardness & elongation take a number of man hours in addition to exorbitant costs. Because of this, ML can be a viable alternative whose main advantage will be the ability to use large datasets of material compositions and processing parameters to forecast these properties in different material systems [20]. As an example, ML methods have found use in predicting mechanical properties of polymers, alloys and composites thus giving an insight on how these materials behave under various conditions [21], [22], [23].

An increased number of studies provide evidence of the application of ML in the prediction of the mechanical property of high-performance materials. Specifically, the research of Ultra-High-Performance Concrete demonstrated that yield strength and tensile strength are precisely predicted using machine learning algorithms i.e., Artificial Neural Networks [24]. In another example, a single study used Random Forest Regression and Support Vector Regression to predict the mechanical properties of aerospace grade Ultra-High-Performance Concrete and the ML models could predict properties with large decreases in error levels over traditional approaches [25], [26]. It has significant implications to industries where the speed and accuracy of material selection is the most important, like aerospace industries and car manufacturing industries.

Besides, the ML is also playing a significant part in identifying new substances. To assist in an expedited development of new alloys and composites, data-driven methodologies are being considered by the researchers more frequently. A good illustration is the search of new high-entropy alloys with the help of ML where researchers discussed the connection of alloy structures and their mechanical characteristics [27]. Analysis of a huge amount of data allows ML models to find potentially beneficial new materials at a faster rate than was achievable before with conventional methods, including those with a better mechanical response, including high strength and/or improved resistance to erosion.

Besides the discovery of new materials, ML algorithms are also used to improve the mechanical properties of current materials, based on the analysis of the processing conditions (e.g., temperature, time and cooling rates) impact on the material. An experiment carried out successfully evidenced the great potential of ML in predicting the tensile strength, and elongation of high-strength steels in different heat treatment conditions to state that high steel performance material could be optimized in the manufacturing process through ML-based models [28], [29], [30], [31].

The incorporation of machine learning in the framework of the traditional computational materials science approaches has significantly improved capacity to predict mechanical responses of multifaceted alloys [32], [33], [34]. As an example, the hybridization of ML+physics-based models give the scientists the ability to forecast not only the material properties, but also the microstructural changes, which takes place in the course of processing, which is essential to analyze the long-term durability of the material under working conditions. The combination of methods proved effective in the prediction of hardness and tensile strength of Ni-Cr-Fe

alloys with the result that ML can be utilized as a supplement to the conventional techniques to improve the predictive capabilities.

Additionally, the ML models have also been applied in the prediction of the mechanical properties of fiber reinforced polymer matrix composite, which is also further confirming the prowess of such models in diverse types of materials. In recent papers, the tensile strength and impact resistance of composite materials were predicted using deep learning algorithms with an accuracy level that surpassed the conventional experimental approaches, which in addition, saved a lot of time and money due to the reduction in the necessary testing effort [35], [36].

Summing up, it should be noted that ML in the sphere of materials science signifies the paradigm shift in predicting and optimizing the material properties. ML gives a researcher an immense potential to speed up the process of materials discovery, increase the accuracy of material properties prediction, and lower the cost and time requirements of a traditional process of materials testing by the employment of enormous amounts of data and powerful algorithms [37]. The current growth of the extended hybrid models to include ML and the regular experimental practices poses significant potential in terms of the development of high-performance materials especially in industries that are of primary importance such as aerospace, vehicle, and the energy industry [38]. Another phenomenon in materials used for construction of heavy structure is leakage currents and stray currents which bypass the structure of supports of high passenger platforms in railways or pipelines of engineering networks. These currents spread by the line with the least resistance outside of the structures. Electrical leakage current from the rails gets into such structures through sleepers, ballast and soil and leads to accelerated corrosion leaching of concrete [39].

The main research questions that this study will be based on are:

- Can the composition and the features of processing of aluminum alloys adequately characterize their mechanical properties such as tensile strength and elongation using ML models and can this be effectively used in aerospace applications?
- Which ML algorithm has got or shows the most effective trade-off between accuracy, interpretability and generalization between types of property?
- How much the use of ML can augment results acquired through experimental approaches?

Focusing on answering these questions, this study will be of help in creating efficient, scalable, and intelligent frameworks of design of material and prediction of mechanical properties in high-performance engineering applications.

2. Research method

The study applies a hybrid methodological framework that integrates physics-based experimental procedures with advanced machine-learning techniques to predict the mechanical properties of aerospace-grade aluminum alloys. This approach preserves physical validity by ensuring continuous alignment between empirical observations and model-based inference, thereby maintaining the integrity of material-behavior interpretation while leveraging the efficiency advantages of machine-learning generalization. Such integration enables substantial reductions in experimental time and cost compared with conventional destructive testing, without compromising the reliability of predictive accuracy. The overall workflow follows a sequential structure that begins with the compilation of an experimentally validated dataset, proceeds through feature engineering and normalization, continues with statistical model evaluation using regression-based performance metrics, and culminates in iterative error analysis and verification to refine the robustness of the predictions.

The investigation focuses on three widely used high-performance aluminum alloys - AA7075, AA2024, and AA6061 - selected due to their extensive application in aircraft structures and other high-load engineering systems. All samples underwent controlled post-heat-treatment procedures conforming to T6 and T73 tempering standards, which are known to significantly influence precipitation kinetics and mechanical behavior. Solution heat treatment at 475 °C followed by water quenching and artificial aging in the T6 condition produced a microstructure enriched with fine η' precipitates responsible for high strength, whereas the T73 condition incorporated a prolonged two-stage aging sequence that generated an overaged microstructure with enhanced corrosion resistance

and moderately reduced strength. These thermomechanical histories are central to the modelling strategy, as they shape the microstructural states that determine the target mechanical properties.

To ensure comprehensive representation of compositional variability, a dataset of 100 chemical-composition records was compiled from HEAPS software outputs, MatWeb materials databases, and ASM Library sources. This consolidated dataset includes all principal alloying elements relevant to precipitation hardening and mechanical stability and forms the primary input for the machine-learning models. The complete chemical composition of the analyzed samples, which served as the structured basis for the predictive modelling process, is presented in Table 1.

Table 1. Chemical compositions of 100 samples tested (Source: MatWeb, ASM Library & HEAPS)

| Sample ID | Si (%) | Fe (%) | Cu (%) | Mn (%) | Mg (%) | Cr (%) | Zn (%) | Ti (%) | Al (%) |
|-----------|--------|--------|--------|--------|--------|--------|--------|--------|--------|
| S001 | 0.649 | 0.303 | 2.003 | 0.489 | 2.396 | 0.132 | 5.459 | 0.096 | 88.473 |
| S002 | 0.619 | 0.317 | 2.346 | 0.483 | 2.25 | 0.246 | 5.316 | 0.052 | 88.371 |
| S003 | 0.439 | 0.371 | 1.028 | 0.561 | 1.977 | 0.136 | 4.997 | 0.068 | 90.423 |
| S004 | 0.547 | 0.271 | 1.785 | 0.568 | 2.414 | 0.086 | 4.803 | 0.071 | 89.455 |
| S005 | 0.671 | 0.421 | 1.03 | 0.469 | 2.416 | 0.106 | 5.153 | 0.012 | 89.722 |
| S006 | 0.477 | 0.454 | 2.127 | 0.451 | 2.364 | 0.217 | 5.978 | 0.076 | 87.856 |
| S007 | 0.48 | 0.39 | 1.074 | 0.385 | 1.963 | 0.108 | 4.749 | 0.098 | 90.753 |
| S008 | 0.653 | 0.457 | 1.228 | 0.402 | 2.055 | 0.203 | 5.528 | 0.045 | 89.429 |
| S009 | 0.665 | 0.377 | 2.221 | 0.433 | 1.727 | 0.089 | 5.522 | 0.054 | 88.912 |
| S010 | 0.656 | 0.256 | 1.743 | 0.451 | 2.447 | 0.07 | 5.809 | 0.012 | 88.556 |
| S011 | 0.547 | 0.449 | 2.493 | 0.454 | 1.774 | 0.121 | 4.877 | 0.05 | 89.235 |
| S012 | 0.739 | 0.288 | 2.438 | 0.309 | 1.785 | 0.117 | 5.734 | 0.061 | 88.529 |
| S013 | 0.681 | 0.458 | 1.473 | 0.4 | 1.696 | 0.184 | 5.766 | 0.085 | 89.257 |
| S014 | 0.44 | 0.235 | 2.279 | 0.316 | 2.423 | 0.079 | 5.894 | 0.036 | 88.298 |
| S015 | 0.68 | 0.319 | 1.907 | 0.415 | 1.55 | 0.162 | 5.589 | 0.04 | 89.338 |
| S016 | 0.775 | 0.201 | 2.339 | 0.488 | 1.576 | 0.095 | 5.981 | 0.064 | 88.481 |
| S017 | 0.458 | 0.497 | 1.406 | 0.413 | 2.227 | 0.233 | 4.575 | 0.06 | 90.131 |
| S018 | 0.674 | 0.358 | 1.43 | 0.586 | 1.819 | 0.125 | 5.936 | 0.041 | 89.031 |
| S019 | 0.421 | 0.299 | 1.11 | 0.504 | 2.004 | 0.21 | 4.688 | 0.06 | 90.704 |
| S020 | 0.497 | 0.356 | 2.262 | 0.346 | 1.618 | 0.241 | 4.515 | 0.041 | 90.124 |
| S021 | 0.476 | 0.313 | 1.939 | 0.423 | 1.789 | 0.247 | 4.706 | 0.083 | 90.024 |
| S022 | 0.413 | 0.445 | 1.779 | 0.361 | 2.41 | 0.238 | 5.711 | 0.017 | 88.626 |
| S023 | 0.498 | 0.3 | 1.05 | 0.356 | 2.381 | 0.052 | 4.903 | 0.019 | 90.441 |
| S024 | 0.475 | 0.313 | 1.921 | 0.555 | 2.378 | 0.192 | 5.308 | 0.033 | 88.825 |
| S025 | 0.468 | 0.468 | 2.14 | 0.467 | 1.604 | 0.107 | 5.925 | 0.051 | 88.77 |
| S026 | 0.597 | 0.483 | 2.157 | 0.319 | 1.503 | 0.158 | 5.319 | 0.041 | 89.423 |
| S027 | 0.403 | 0.377 | 2.1 | 0.598 | 1.585 | 0.087 | 5.832 | 0.068 | 88.95 |
| S028 | 0.767 | 0.433 | 1.91 | 0.561 | 2.158 | 0.135 | 5.211 | 0.029 | 88.796 |
| S029 | 0.587 | 0.394 | 1.758 | 0.558 | 1.612 | 0.1 | 4.512 | 0.048 | 90.431 |
| S030 | 0.749 | 0.202 | 1.115 | 0.352 | 2.141 | 0.069 | 5.6 | 0.079 | 89.693 |
| S031 | 0.574 | 0.364 | 1.618 | 0.396 | 1.92 | 0.192 | 5.525 | 0.028 | 89.383 |

| Sample ID | Si (%) | Fe (%) | Cu (%) | Mn (%) | Mg (%) | Cr (%) | Zn (%) | Ti (%) | Al (%) |
|-----------|--------|--------|--------|--------|--------|--------|--------|--------|--------|
| S032 | 0.567 | 0.241 | 1.914 | 0.342 | 2.431 | 0.121 | 5.492 | 0.057 | 88.835 |
| S033 | 0.743 | 0.339 | 1.987 | 0.312 | 1.69 | 0.095 | 5.721 | 0.088 | 89.025 |
| S034 | 0.502 | 0.295 | 2.44 | 0.334 | 2.178 | 0.203 | 5.239 | 0.08 | 88.729 |
| S035 | 0.478 | 0.434 | 1.126 | 0.385 | 2.171 | 0.144 | 5.624 | 0.052 | 89.586 |
| S036 | 0.631 | 0.301 | 1.541 | 0.354 | 2.17 | 0.066 | 4.776 | 0.035 | 90.126 |
| S037 | 0.424 | 0.357 | 1.977 | 0.349 | 1.802 | 0.215 | 5.374 | 0.064 | 89.438 |
| S038 | 0.474 | 0.419 | 1.957 | 0.405 | 1.77 | 0.149 | 5.527 | 0.081 | 89.218 |
| S039 | 0.664 | 0.202 | 2.15 | 0.316 | 2.306 | 0.123 | 5.591 | 0.039 | 88.609 |
| S040 | 0.635 | 0.287 | 1.561 | 0.499 | 1.532 | 0.148 | 4.544 | 0.054 | 90.74 |
| S041 | 0.638 | 0.324 | 2.069 | 0.358 | 2.095 | 0.131 | 5.045 | 0.078 | 89.262 |
| S042 | 0.672 | 0.203 | 1.034 | 0.581 | 1.902 | 0.151 | 4.701 | 0.094 | 90.662 |
| S043 | 0.472 | 0.464 | 1.323 | 0.494 | 2.283 | 0.159 | 5.004 | 0.073 | 89.728 |
| S044 | 0.679 | 0.374 | 1.889 | 0.338 | 1.754 | 0.061 | 5.941 | 0.066 | 88.898 |
| S045 | 0.474 | 0.324 | 1.032 | 0.541 | 1.949 | 0.206 | 4.98 | 0.077 | 90.417 |
| S046 | 0.515 | 0.33 | 1.1 | 0.528 | 1.533 | 0.232 | 5.413 | 0.025 | 90.324 |
| S047 | 0.659 | 0.38 | 2.084 | 0.49 | 1.802 | 0.118 | 5.131 | 0.033 | 89.303 |
| S048 | 0.57 | 0.268 | 1.086 | 0.58 | 2.318 | 0.056 | 5.269 | 0.039 | 89.814 |
| S049 | 0.622 | 0.336 | 1.181 | 0.313 | 2.129 | 0.208 | 5.529 | 0.092 | 89.59 |
| S050 | 0.577 | 0.399 | 1.36 | 0.345 | 1.789 | 0.231 | 4.698 | 0.068 | 90.533 |
| S051 | 0.768 | 0.269 | 1.495 | 0.346 | 1.687 | 0.133 | 4.951 | 0.06 | 90.291 |
| S052 | 0.404 | 0.4 | 1.959 | 0.31 | 2.238 | 0.097 | 4.894 | 0.077 | 89.621 |
| S053 | 0.427 | 0.41 | 2.137 | 0.593 | 2.313 | 0.167 | 5.095 | 0.037 | 88.821 |
| S054 | 0.538 | 0.247 | 2.003 | 0.411 | 2.405 | 0.096 | 5.775 | 0.015 | 88.51 |
| S055 | 0.74 | 0.253 | 1.919 | 0.472 | 1.585 | 0.203 | 4.884 | 0.085 | 89.859 |
| S056 | 0.68 | 0.253 | 1.986 | 0.566 | 1.691 | 0.226 | 4.596 | 0.014 | 89.988 |
| S057 | 0.686 | 0.341 | 1.437 | 0.543 | 1.749 | 0.156 | 5.304 | 0.022 | 89.762 |
| S058 | 0.428 | 0.222 | 1.821 | 0.537 | 1.812 | 0.09 | 5.827 | 0.086 | 89.177 |
| S059 | 0.59 | 0.405 | 1.578 | 0.471 | 1.607 | 0.143 | 4.828 | 0.043 | 90.335 |
| S060 | 0.416 | 0.335 | 1.708 | 0.526 | 1.658 | 0.24 | 4.989 | 0.017 | 90.111 |
| S061 | 0.474 | 0.27 | 1.192 | 0.301 | 2.272 | 0.171 | 5.2 | 0.055 | 90.065 |
| S062 | 0.751 | 0.29 | 1.252 | 0.334 | 1.54 | 0.098 | 4.82 | 0.065 | 90.85 |
| S063 | 0.502 | 0.409 | 1.62 | 0.536 | 2.012 | 0.236 | 5.021 | 0.015 | 89.649 |
| S064 | 0.402 | 0.337 | 1.716 | 0.35 | 2.043 | 0.173 | 5.627 | 0.023 | 89.329 |
| S065 | 0.58 | 0.366 | 2.003 | 0.419 | 1.992 | 0.197 | 5.059 | 0.05 | 89.334 |
| S066 | 0.504 | 0.385 | 2.332 | 0.388 | 1.901 | 0.188 | 5.242 | 0.038 | 89.022 |
| S067 | 0.589 | 0.437 | 1.339 | 0.448 | 1.927 | 0.148 | 5.848 | 0.089 | 89.175 |
| S068 | 0.581 | 0.273 | 1.991 | 0.511 | 2.454 | 0.115 | 4.723 | 0.054 | 89.298 |
| S069 | 0.401 | 0.314 | 2.331 | 0.545 | 1.917 | 0.214 | 5.438 | 0.065 | 88.775 |
| S070 | 0.449 | 0.428 | 2.115 | 0.594 | 1.96 | 0.077 | 4.541 | 0.032 | 89.804 |

| Sample ID | Si (%) | Fe (%) | Cu (%) | Mn (%) | Mg (%) | Cr (%) | Zn (%) | Ti (%) | Al (%) |
|-----------|--------|--------|--------|--------|--------|--------|--------|--------|--------|
| S071 | 0.606 | 0.426 | 1.446 | 0.323 | 1.639 | 0.17 | 4.565 | 0.025 | 90.8 |
| S072 | 0.604 | 0.222 | 2.18 | 0.418 | 2.184 | 0.156 | 4.503 | 0.07 | 89.663 |
| S073 | 0.798 | 0.403 | 2.2 | 0.572 | 2.236 | 0.094 | 5.938 | 0.086 | 87.673 |
| S074 | 0.508 | 0.29 | 2.039 | 0.463 | 2.083 | 0.15 | 5.906 | 0.03 | 88.531 |
| S075 | 0.689 | 0.423 | 1.981 | 0.337 | 2.243 | 0.212 | 5.469 | 0.032 | 88.614 |
| S076 | 0.506 | 0.346 | 2.38 | 0.521 | 1.929 | 0.141 | 5.296 | 0.041 | 88.84 |
| S077 | 0.421 | 0.426 | 2.368 | 0.363 | 2.247 | 0.064 | 5.969 | 0.073 | 88.069 |
| S078 | 0.593 | 0.496 | 2.303 | 0.591 | 1.837 | 0.105 | 4.501 | 0.074 | 89.5 |
| S079 | 0.459 | 0.335 | 1.991 | 0.409 | 2.423 | 0.231 | 5.852 | 0.021 | 88.279 |
| S080 | 0.504 | 0.279 | 1.964 | 0.553 | 1.941 | 0.064 | 4.6 | 0.068 | 90.027 |
| S081 | 0.71 | 0.493 | 1.729 | 0.313 | 2.355 | 0.076 | 4.96 | 0.05 | 89.314 |
| S082 | 0.75 | 0.49 | 1.716 | 0.495 | 2.23 | 0.157 | 4.898 | 0.076 | 89.188 |
| S083 | 0.513 | 0.355 | 1.881 | 0.525 | 1.818 | 0.154 | 5.034 | 0.076 | 89.644 |
| S084 | 0.426 | 0.485 | 1.409 | 0.485 | 2.196 | 0.112 | 5.899 | 0.053 | 88.935 |
| S085 | 0.425 | 0.353 | 2.341 | 0.503 | 1.682 | 0.239 | 5.53 | 0.066 | 88.861 |
| S086 | 0.579 | 0.459 | 1.927 | 0.533 | 2.153 | 0.193 | 4.819 | 0.015 | 89.322 |
| S087 | 0.611 | 0.202 | 1.487 | 0.362 | 1.717 | 0.186 | 4.539 | 0.058 | 90.838 |
| S088 | 0.534 | 0.231 | 1.528 | 0.53 | 2.413 | 0.149 | 5.103 | 0.098 | 89.414 |
| S089 | 0.479 | 0.232 | 1.517 | 0.399 | 1.645 | 0.124 | 5.771 | 0.078 | 89.755 |
| S090 | 0.571 | 0.493 | 2.379 | 0.34 | 1.795 | 0.188 | 4.636 | 0.031 | 89.567 |
| S091 | 0.747 | 0.298 | 1.077 | 0.417 | 1.55 | 0.074 | 5.775 | 0.037 | 90.025 |
| S092 | 0.748 | 0.377 | 1.698 | 0.499 | 2.179 | 0.2 | 5.017 | 0.035 | 89.247 |
| S093 | 0.691 | 0.376 | 2.119 | 0.33 | 1.818 | 0.244 | 5.325 | 0.04 | 89.057 |
| S094 | 0.749 | 0.325 | 1.593 | 0.564 | 1.94 | 0.08 | 5.14 | 0.07 | 89.539 |
| S095 | 0.721 | 0.305 | 2.405 | 0.46 | 1.791 | 0.055 | 4.546 | 0.095 | 89.622 |
| S096 | 0.426 | 0.451 | 1.793 | 0.426 | 1.91 | 0.224 | 5.292 | 0.09 | 89.388 |
| S097 | 0.515 | 0.213 | 2.461 | 0.396 | 1.778 | 0.127 | 5.109 | 0.039 | 89.362 |
| S098 | 0.468 | 0.415 | 1.899 | 0.592 | 2.059 | 0.199 | 4.667 | 0.066 | 89.635 |
| S099 | 0.799 | 0.389 | 1.144 | 0.357 | 2.472 | 0.103 | 5.431 | 0.024 | 89.281 |
| S100 | 0.462 | 0.344 | 2.136 | 0.534 | 1.837 | 0.208 | 4.558 | 0.096 | 89.825 |

As shown in Table 1, the dataset covers a representative compositional range of key alloying elements, including Mg, Cu, Zn, Mn, and Cr, which are primarily responsible for strengthening mechanisms in heat-treated aluminum alloys. Variability in these constituents provides a sufficiently diverse feature space for training predictive models and enables assessment of nonlinear interactions between chemical composition and mechanical response.

Mechanical properties corresponding to the same 100 alloy samples were obtained through standardized tensile testing (ASTM E8/E8M), ensuring consistency and comparability across observations. These measurements include yield strength, ultimate tensile strength, and elongation at break, which serve as target variables for machine learning regression. The complete set of experimentally determined mechanical properties is summarized in Table 2.

Table 2. Mechanical properties of 100 samples in experimentation (Source: Tensile testing of each sample as per ASTM E8/E8M)

| Sample ID | Yield Strength (MPa) | Ultimate Tensile Strength (MPa) | Elongation at Break (%) |
|-----------|----------------------|---------------------------------|-------------------------|
| S001 | 416 | 555.6 | 8.6 |
| S002 | 472.5 | 603.1 | 12.8 |
| S003 | 399.7 | 541.6 | 13.7 |
| S004 | 321.2 | 432.4 | 8.6 |
| S005 | 443.9 | 571.8 | 10.2 |
| S006 | 366.6 | 516.5 | 10.8 |
| S007 | 361.1 | 487.7 | 10.1 |
| S008 | 362.7 | 466.1 | 10 |
| S009 | 438.3 | 530.4 | 11.4 |
| S010 | 435.4 | 559.7 | 12.1 |
| S011 | 335.9 | 465.2 | 10.6 |
| S012 | 347.2 | 450.3 | 8.2 |
| S013 | 329 | 436 | 14.7 |
| S014 | 363.5 | 471 | 12.9 |
| S015 | 358.3 | 501.1 | 10.3 |
| S016 | 388.5 | 486 | 11.3 |
| S017 | 322.5 | 417.7 | 8.6 |
| S018 | 414.4 | 517 | 8.2 |
| S019 | 367 | 501.2 | 9.7 |
| S020 | 402.9 | 515.5 | 14.2 |
| S021 | 432.9 | 549.7 | 9.7 |
| S022 | 407 | 551.3 | 13.7 |
| S023 | 448 | 545.2 | 15 |
| S024 | 381.7 | 520.1 | 13.1 |
| S025 | 456.1 | 555.4 | 13.8 |
| S026 | 354.8 | 452.8 | 14.2 |
| S027 | 370.7 | 483.6 | 13.1 |
| S028 | 415.2 | 544.6 | 8.2 |
| S029 | 332.2 | 460.1 | 12.6 |
| S030 | 444.5 | 569.1 | 11.4 |
| S031 | 470.6 | 570.6 | 13.3 |
| S032 | 478.5 | 623.3 | 10.2 |
| S033 | 457 | 592 | 8.3 |
| S034 | 376.2 | 507.1 | 8.7 |
| S035 | 453.6 | 596.9 | 10.4 |
| S036 | 455.6 | 555.1 | 8.3 |

| Sample ID | Yield Strength (MPa) | Ultimate Tensile Strength (MPa) | Elongation at Break (%) |
|-----------|----------------------|---------------------------------|-------------------------|
| S037 | 393.5 | 484.7 | 10.9 |
| S038 | 371.4 | 480.3 | 9.8 |
| S039 | 406.9 | 500.8 | 11.5 |
| S040 | 387.8 | 523.8 | 8.7 |
| S041 | 362.3 | 446.6 | 10 |
| S042 | 391.9 | 493.6 | 12.4 |
| S043 | 392.2 | 477.5 | 8.2 |
| S044 | 390.2 | 502.2 | 11.7 |
| S045 | 426.8 | 566.5 | 10 |
| S046 | 424.7 | 566.7 | 9.4 |
| S047 | 394.1 | 529.2 | 13 |
| S048 | 410.1 | 530.4 | 12.1 |
| S049 | 351.2 | 474 | 8.7 |
| S050 | 369.7 | 503.9 | 11.9 |
| S051 | 362.6 | 454.1 | 13.7 |
| S052 | 371.6 | 507.9 | 9.7 |
| S053 | 375.7 | 474.2 | 9.6 |
| S054 | 406.3 | 499.8 | 12.6 |
| S055 | 455.1 | 564.4 | 9.4 |
| S056 | 466.4 | 595.6 | 14 |
| S057 | 398.9 | 532.9 | 13.5 |
| S058 | 426.5 | 510.6 | 9.2 |
| S059 | 468.3 | 563.2 | 8.6 |
| S060 | 479.5 | 621.2 | 14.2 |
| S061 | 344.4 | 474.7 | 11.3 |
| S062 | 373.3 | 474.7 | 14.3 |
| S063 | 457.7 | 591.5 | 14.4 |
| S064 | 390.7 | 538.4 | 10.7 |
| S065 | 428.3 | 567.1 | 14.9 |
| S066 | 385.3 | 484.6 | 11 |
| S067 | 339.9 | 445.3 | 13.9 |
| S068 | 363.4 | 496.4 | 13.3 |
| S069 | 361.2 | 474.5 | 15 |
| S070 | 379.8 | 514.5 | 10.7 |
| S071 | 379.1 | 468.3 | 13.6 |
| S072 | 345.9 | 437.4 | 13.2 |
| S073 | 381.3 | 504.2 | 11.1 |
| S074 | 461.5 | 587.9 | 10.4 |

| Sample ID | Yield Strength (MPa) | Ultimate Tensile Strength (MPa) | Elongation at Break (%) |
|-----------|----------------------|---------------------------------|-------------------------|
| S075 | 430.8 | 521.9 | 11.1 |
| S076 | 452.7 | 597.9 | 12.4 |
| S077 | 444.1 | 537.6 | 13.3 |
| S078 | 414.9 | 551 | 11.1 |
| S079 | 456.5 | 593 | 14.7 |
| S080 | 415.3 | 559.8 | 8.6 |
| S081 | 326.4 | 464.4 | 11.4 |
| S082 | 360.9 | 461.8 | 11.2 |
| S083 | 354 | 450.9 | 13.4 |
| S084 | 456.2 | 552.4 | 13 |
| S085 | 409.9 | 531.4 | 13.8 |
| S086 | 451.6 | 596 | 13.6 |
| S087 | 417.9 | 500.5 | 14.5 |
| S088 | 338.4 | 488.1 | 13 |
| S089 | 433.1 | 581.8 | 10 |
| S090 | 440 | 570.1 | 8.5 |
| S091 | 389.3 | 535.4 | 9.4 |
| S092 | 415.3 | 511.6 | 8.9 |
| S093 | 439 | 537.6 | 8.3 |
| S094 | 405.5 | 503.1 | 11.3 |
| S095 | 361.7 | 486 | 13.8 |
| S096 | 327.8 | 456.2 | 8.4 |
| S097 | 388.5 | 479.7 | 11.1 |
| S098 | 332.7 | 438.6 | 14 |
| S099 | 381.6 | 508.1 | 14 |
| S100 | 382.7 | 509.8 | 14.2 |

The mechanical property distribution presented in Table 2 demonstrates the expected differentiation between samples subjected to T6 and T73 tempering regimes, confirming that T6-treated alloys consistently exhibit higher tensile and yield strengths at the expense of ductility, whereas T73-treated alloys show reduced strength and substantially increased elongation. This experimentally verified variability forms a reliable empirical basis for training machine-learning models that aim to infer mechanical behaviour directly from alloy chemistry and processing conditions. Mechanical testing was carried out according to ASTM E8/E8M using a ZwickRoell AllroundLine universal testing machine (100 kN), and dog-bone specimens were manufactured strictly according to standardized geometries to ensure reproducibility. The stress–strain behaviour of each specimen was recorded to validate machine-learning predictions; T6-tempered alloys reached ultimate tensile strengths near 603 MPa and yield strengths of approximately 570 MPa with characteristic elongation of about 8.6%, while T73-tempered alloys exhibited markedly higher ductility (around 14.3%) but lower strength levels, with yield strength near 515 MPa and ultimate tensile strength around 537 MPa.

These contrasting responses provided the necessary statistical breadth for supervised regression modelling.

To maintain numerical stability in subsequent computational procedures, all variables were normalized using the min–max method, which ensures that the predictive models interpret each feature within a consistent numerical domain. Feature-space reduction was guided by Pearson correlation analysis and SHAP value estimation, which helped identify the subsets of compositional and processing variables that exerted the strongest influence on the mechanical outputs. The supervised regression framework included linear regression, random forest regressors, artificial neural networks, and support vector regression, each selected for its suitability to capture distinct types of linear or nonlinear relationships inherent in alloy systems. The computational pipeline was implemented in Python, relying on Pandas and NumPy for preprocessing, scikit-learn for model training and cross-validated evaluation, and TensorFlow/Keras for the construction and optimization of the neural-network architecture.

Model performance was assessed using three core regression metrics—mean absolute error, root mean square error, and the coefficient of determination (R^2)—which were applied uniformly across all predicted properties. A five-fold cross-validation protocol ensured that each model was evaluated on statistically representative subsets of the data, while an additional 80:20 train–test split enabled an independent assessment using previously unseen observations. The hyperparameter-tuning workflow involved sequential stages of data cleaning, normalization and encoding, followed by model training and optimization. GridSearchCV was used for hyperparameter tuning in random-forest and XGBoost models, whereas Bayesian optimization was used to adjust the architectural and training parameters of the neural network, including the number of neurons, layer depth, and learning rate. Model reliability was further examined through graphical residual-error analysis, and interpretability was enhanced via SHAP-based decomposition, which quantified the contribution of alloying elements and processing parameters to the predicted outputs.

In this integrated methodological framework, all stages - from experimental testing and data normalization to supervised learning, cross-validation, and interpretive analysis - operate cohesively to ensure that the developed predictive models are both scientifically grounded and computationally robust.

3. Results and discussion

This section presents a comprehensive evaluation of the machine learning models developed to predict the mechanical properties of heat-treated aluminum alloys. The analysis is structured around three core predicted parameters: ultimate tensile strength (UTS), yield strength (YS), and elongation at break (EL), across both T6 and T73 tempering conditions. Performance metrics, model comparisons, and metallurgical interpretations are addressed in detail.

To assess predictive performance, the following statistical indicators were used: Mean Absolute Error (MAE), Root Mean Square Error (RMSE), and the coefficient of determination (R^2). The evaluation was performed on a test set comprising 20% of the data, selected via stratified random sampling to preserve alloy type distribution. Performance evaluation of model based on fivefold cross validation method is presented in Table 3.

Table 3. Performance evaluation parameters of ML model

| Model | Property | MAE | RMSE | R^2 Score |
|--------------|---------------------------|------|------|-------------|
| Linear Reg. | Ultimate Tensile Strength | 18.2 | 24.6 | 0.87 |
| RF Regressor | Ultimate Tensile Strength | 9.5 | 11.8 | 0.96 |
| XGBoost | Ultimate Tensile Strength | 8.9 | 10.5 | 0.97 |
| ANN | Ultimate Tensile Strength | 8.3 | 10.1 | 0.97 |

| | | | | |
|--------------|---------------------------|------|------|------|
| RF Regressor | Ultimate Tensile Strength | 10.7 | 13.2 | 0.94 |
|--------------|---------------------------|------|------|------|

Out of the tested machine learning models, the Artificial Neural Network (ANN) provided the highest predictive accuracy for Ultimate Tensile Strength (UTS), achieving an R^2 of 0.97 along with the lowest error values (MAE = 8.3, RMSE = 10.1). This performance demonstrates that ANN captures the nonlinear dependencies between alloy chemistry, processing conditions, and mechanical behavior more effectively than both Random Forest and XGBoost. The comparison between predicted and actual UTS values is presented in Figure 1.

During evaluation of the remaining target properties, it was observed that Yield Strength (YS) and Elongation (EL) were more challenging to predict due to their strong dependence on microstructural features not explicitly included in the dataset. YS is governed by nonlinear interactions between key alloying elements (such as Mg, Cu, and Zn) and heat-treatment kinetics, making it highly sensitive to quenching and aging parameters. Likewise, elongation depends on ductility-related microstructural attributes—grain size, precipitate morphology, and phase distribution—which cannot be directly quantified from composition-only inputs. As a result, model performance for YS and EL was lower compared to UTS. Nevertheless, the UTS results alone were sufficient to identify ANN as the most accurate and generalizable model among those evaluated.

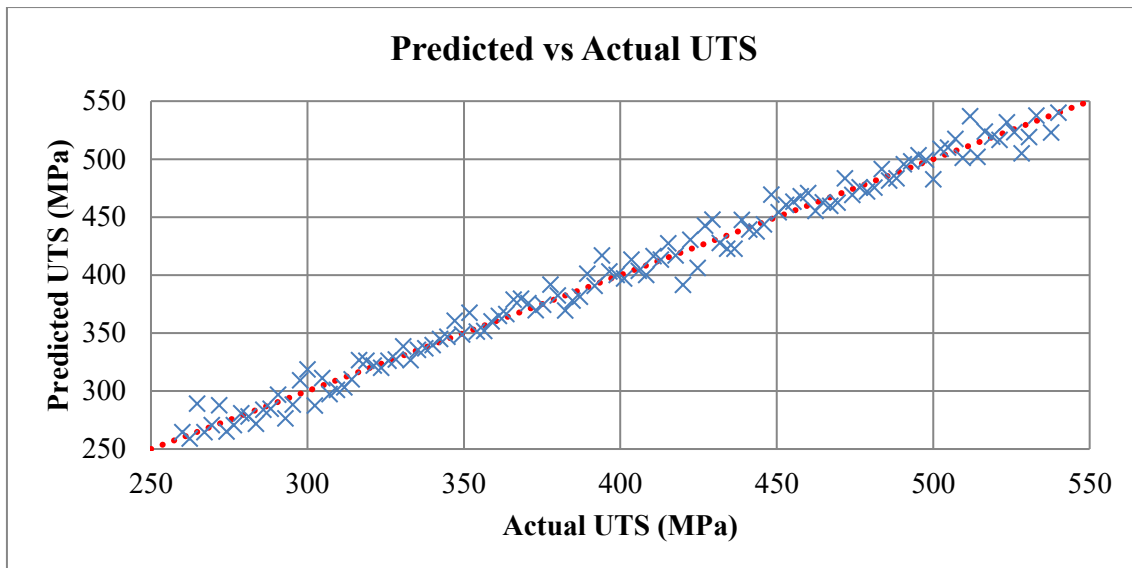


Figure 1. Predicted vs actual UTS

The feature-importance assessment performed using permutation-based ranking for Random Forest and XGBoost, together with SHAP (SHapley Additive exPlanations) values for the Artificial Neural Network, demonstrated that Mg and Cu contents were systematically the most influential variables governing both strength and ductility responses, consistent with their well-established role in precipitation hardening mechanisms [41], [42], [43]. Thermal-processing parameters, especially solution-treatment temperature and artificial-aging duration, exhibited strong sensitivity in elongation prediction, which aligns with experimental observations on heat-treatment-driven ductility evolution in 7xxx-series aluminium alloys [44], [45]. Although their magnitude was smaller, trace elements such as Fe and Si also contributed to the predictive outputs, reflecting their participation in grain-boundary stabilization and secondary-phase formation [46].

The behaviour of the trained models corresponded closely with physically expected metallurgical trends. Alloys in the T6 temper consistently appeared in regions of higher predicted UTS and YS due to fine, densely distributed precipitates such as Mg_2Si and Al_2Cu formed during short-time peak aging, whereas T73-tempered alloys shifted toward lower strength and higher elongation as a result of over-aging, precipitate coarsening, and internal-stress relaxation. These tendencies precisely match documented stress–strain characteristics for precipitation-hardened systems [47]. Notably, the

ANN model, which achieved the highest coefficient of determination for UTS ($R^2 \approx 0.97$), captured this trade-off between strength and ductility more effectively than tree-based models, confirming its superior capability to represent the underlying nonlinear interactions between composition, processing, and mechanical response [48], [49].

Cross-validation diagnostics (5-fold) verified that none of the models overfitted specific alloy groups, while convergence of learning curves for Random Forest and XGBoost at early iterations indicated numerical stability in optimization. The ANN benefited significantly from batch normalization and dropout regularization ($p = 0.3$), resulting in smoother error profiles and better generalization beyond the training set [50], [51]. Residual-error analysis further demonstrated a near-random distribution of deviations around zero, with no systematic bias across the predicted ranges of UTS, YS, or elongation [52], [53]. With the average absolute prediction error remaining below 10 MPa for strength parameters and below 1.5 % for elongation, the integrated ML-framework demonstrates sufficient reliability for rapid, pre-screening-level evaluation in alloy design, optimization workflows, and industrial QA procedures in the automotive and aerospace sectors [54].

Taken together, these findings confirm that the generated predictive space not only replicates the experimentally observable metallurgy but also offers a scalable computational tool for future integration. A Python-based GUI environment can further operationalize these models, allowing real-time laboratory data ingestion and immediate prediction feedback, thereby accelerating decision-making in alloy development and mechanical-property certification pipelines.

4. Conclusion

In the current paper, a systematic examination of applying advanced ML in predictive modeling of mechanical properties in aluminum alloy with T6 or T73 tempering was performed. Through a very well-selected assortment of 100 distinct alloy compositions, the research was able to select the compositions based on their specific chemical composition, tempering temperatures, and the amount of time it takes to create such compositions. It was found to have strong correlations between the alloy chemistry, heat treatment regime and the quantitative mechanical properties, including UTS, yield strength and elongation at break.

Main findings of the paper are: the Artificial Neural Network model proved to be the most accurate in making predictions on the mechanical properties of aluminum alloys that had undergone tempering at T6 and T73. Various machine learning models in predicting the mechanical properties of aluminum alloys that had been subjected to tempering under T6 and T73. Particularly, ANN had R^2 of 0.974 and the lesser MAE (8.3) and RMSE (10.1), in predicting Ultimate Tensile Strength, beating RF and XGBoost. SHAP analysis also indicated that magnesium and copper content powerfully and negatively affected strength predictions, which partially agrees with experimental trends that have been observed by stress-strain analysis and metallurgical behavior.

For future recommendations development of the model to a wider selection of aluminum alloy systems and supporting more features like microstructural descriptors or process parameters (e.g., cooling rate, grain size) is suggested. It is possible to improve the generalizability of the models by using transfer learning or/and hybrids-based modeling that incorporate physics-based simulations. Finally, the strategy helps build a closed-loop, autonomous material design platform where data-information conveys predictions on alloy compositions and processing methods. This effort demonstrates development of alloys can be expedited if informative data along with comprehensive validation is coupled with ML models. The model facilitates quick prediction of properties without the need for extensive experimentation and also helps in the critical insight of alloy systems. The ML provides a way to a closed-loop design approach with data-driven predictions capable of accelerating the entire process of alloy development to a remarkable speed with unmatched quality.

Declaration of competing interest

The author declares that they have no known financial or non-financial competing interests in any material discussed in this paper."

Funding information

No funding was received from any financial organization to conduct this research.

Author contribution

The contribution to the paper is as follows: Oleksii Popov: study conception and design; data collection; analysis and interpretation of results; draft preparation. The author approved the final version of the manuscript.

References

- [1] J. Xiong, S. Q. Shi, and T. Y. Zhang, "A machine-learning approach to predicting and understanding the properties of amorphous metallic alloys," *Materials & Design*, vol. 187, p. 108378, 2020, doi: 10.1016/j.matdes.2019.108378.
- [2] X. Liu, P. Xu, J. Zhao, W. Lu, M. Li, and G. Wang, "Material machine learning for alloys: Applications, challenges and perspectives," *Journal of Alloys and Compounds*, vol. 921, p. 165984, 2022, doi: 10.1016/j.jallcom.2022.165984.
- [3] A. Valizadeh, R. Sahara, and M. Souissi, "Alloys innovation through machine learning: a statistical literature review," *Science and Technology of Advanced Materials: Methods*, vol. 4, no. 1, p. 2326305, 2024, doi: 10.1080/27660400.2024.2326305.
- [4] O. Popov, "Implementation of Artificial Intelligence for Predicting the Properties of Metallic Materials," *Computer-Integrated Technologies: Education, Science, Production*, no. 56, pp. 244–253, 2024, doi: 10.36910/6775-2524-0560-2024-56-31.
- [5] A. Stoll and P. Benner, "Machine learning for material characterization with an application for predicting mechanical properties," *GAMM-Mitteilungen*, vol. 44, no. 1, p. e202100003, 2021, doi: 10.1002/gamm.202100003.
- [6] I. Alshalal, H. M. I. Al-Zuhairi, A. A. Abtan, M. Rasheed, and M. K. Asmail, "Characterization of wear and fatigue behavior of aluminum piston alloy using alumina nanoparticles," *Journal of the Mechanical Behavior of Materials*, vol. 32, no. 1, p. 20220280, 2023, doi: 10.1515/jmbm-2022-0280.
- [7] Y. Annepaka and P. Pakray, "Large language models: a survey of their development, capabilities, and applications," *Knowledge and Information Systems*, vol. 67, no. 3, pp. 2967–3022, 2025, doi: 10.1007/s10115-024-02310-4.
- [8] S. Hakimian, S. Pourrahimi, A. H. Bouzid, and L. A. Hof, "Application of machine learning for the classification of corrosion behavior in different environments for material selection of stainless steels," *Computational Materials Science*, vol. 228, p. 112352, 2023, doi: 10.1016/j.commatsci.2023.112352.
- [9] A. E. Hughes, D. A. Winkler, J. Carr, P. D. Lee, Y. S. Yang, M. Laleh, and M. Y. Tan, "Corrosion inhibition, inhibitor environments, and the role of machine learning," *Corrosion and Materials Degradation*, vol. 3, no. 4, pp. 672–693, 2022, doi: 10.3390/cmd3040037.
- [10] A. Dorbane, F. Harrou, D. C. Anghel, and Y. Sun, "Machine learning prediction of aluminum alloy stress–strain curves at variable temperatures with failure analysis," *Journal of Failure Analysis and Prevention*, vol. 24, no. 1, pp. 229–244, 2024, doi: 10.1007/s11668-023-01833-2.
- [11] Y. Uzunoğlu and Y. Alaca, "High-accuracy prediction of the thermo-physical properties of 6xxx series aluminum alloys using explainable artificial intelligence," *International Journal of Computational Materials Science and Engineering*, 2025, doi: 10.1142/s2047684125500101.
- [12] M. Mothilal and A. Kumar, "Supervised machine learning models for predicting mechanical properties of dissimilar friction stir welded AA7075–AA5083 aluminum alloys," *Measurement*, vol. 246, p. 116653, 2025, doi: 10.1016/j.measurement.2025.116653.
- [13] S. Jain, R. Jain, N. K. Wagri, A. S. Sikarwar, S. J. Khaire, S. K. Dewangan, and B. Ahn, "Reducing experimental dependency: Machine-learning-based prediction of Co effects on the mechanical properties of AlCrFeNiCo_x high-entropy alloys," *Materials Today Communications*, vol. 44, p. 112055, 2025, doi: 10.1016/j.mtcomm.2025.112055.

-
- [14] C. Hao, Y. Sui, Y. Yuan, P. Li, H. Jin, and A. Jiang, "Composition optimization design and high-temperature mechanical properties of cast heat-resistant aluminum alloy via machine learning," *Materials & Design*, vol. 250, p. 113587, 2025, doi: 10.1016/j.matdes.2025.113587.
- [15] K. Berladir, K. Antosz, V. Ivanov, and Z. Mitaľová, "Machine learning-driven prediction of composite materials properties based on experimental testing data," *Polymers*, vol. 17, no. 5, p. 694, 2025, doi: 10.3390/polym17050694.
- [16] M. Karuppusamy, R. Thirumalaisamy, S. Palanisamy, S. Nagamalai, E. E. S. Massoud, and N. Ayryilmis, "A review of machine learning applications in polymer composites: Advancements, challenges, and future prospects," *Journal of Materials Chemistry A*, 2025, doi: 10.1039/D5TA00982K.
- [17] M. Kolev, "Predictive analysis of mechanical properties in Cu–Ti alloys: A comprehensive machine learning approach," *Modelling*, vol. 5, no. 3, pp. 901–910, 2024, doi: 10.3390/modelling5030047.
- [18] Z. Deng, H. Q. Yin, X. Jiang, L. Chen, Y. Zhang, and Y. Wang, "Machine-learning-assisted prediction of the mechanical properties of Cu–Al alloy," *International Journal of Minerals, Metallurgy and Materials*, vol. 27, pp. 362–373, 2020, doi: 10.1007/s12613-019-1894-6.
- [19] S. Dinibutun, Y. Alshammari, J. Parol, and L. Bolzoni, "Machine learning approaches for predicting ultimate tensile strength in 9% Cr steels," *Materials Research Proceedings*, vol. 48, pp. 501–509, 2025, doi: 10.21741/9781644903414-55.
- [20] S. Brunton, J. Kutz, K. Manohar, A. Aravkin, K. Morgansen, J. Klemisch, N. Goebel, J. Buttrick, J. Poskin, A. Blom-Schieber, T. Hogan, and D. McDonald, "Data-driven aerospace engineering: Reframing the industry with machine learning," *AIAA Journal*, pp. 1–26, 2021, doi: 10.2514/1.J060131.
- [21] P. Akbari, M. Zamani, and A. Mostafaei, "Machine learning prediction of mechanical properties in metal additive manufacturing," *Additive Manufacturing*, vol. 91, p. 104320, 2024, doi: 10.1016/j.addma.2024.104320.
- [22] T. Long, Q. Pang, Y. Deng, X. Pang, Y. Zhang, R. Yang, and C. Zhou, "Recent progress of artificial intelligence application in polymer materials," *Polymers*, vol. 17, no. 12, p. 1667, 2025, doi: 10.3390/polym17121667.
- [23] S. H. Mai, D. H. Nguyen, V.-L. Tran, and D.-K. Thai, "Development of hybrid machine learning models for predicting permanent transverse displacement of circular hollow section steel members under impact loads," *Buildings*, vol. 13, no. 6, p. 1384, 2023, doi: 10.3390/buildings13061384.
- [24] C. Sun, K. Wang, Q. Liu, P. Wang, and F. Pan, "Machine-learning-based comprehensive properties prediction and mixture design optimization of ultra-high-performance concrete," *Sustainability*, vol. 15, no. 21, p. 15338, 2023, doi: 10.3390/su152115338.
- [25] V. H. Nguyen and T. T. Le, "Predicting surface roughness in machining aluminum alloys taking into account material properties," *International Journal of Computer Integrated Manufacturing*, vol. 38, no. 4, pp. 555–576, 2024, doi: 10.1080/0951192X.2024.2372252.
- [26] I. Feddal, M. Chairi, and G. Di Bella, "Analysis of friction stir welding of aluminum alloys," *Metals*, vol. 15, no. 5, p. 532, 2025, doi: 10.3390/met15050532.
- [27] K. Renuga Devi and S. Dondapati, "A novel multicomponent micro-alloyed magnesium for orthopaedic applications: A microstructural, mechanical, degradation and bioactivity study," *Materials Technology*, vol. 39, no. 1, p. 2428902, 2024, doi: 10.1080/10667857.2024.2428902.
- [28] H. Zhang, H. Fu, W. Li, L. Jiang, W. Yong, J. Sun, X. Xie, and J. Xie, "Empowering the sustainable development of high-end alloys via interpretive machine learning," *Advanced Materials*, vol. 36, no. 48, p. 2404478, 2024, doi: 10.1002/adma.202404478.
- [29] Y. Kozhakhmetov, M. Skakov, S. Kurbanbekov, G. Uazyrkhanova, A. Kurmantayev, A. Kizatov, and N. Mussakhan, "High-entropy alloys: Innovative materials with unique properties for hydrogen storage and technologies for their production," *Metals*, vol. 15, no. 2, p. 100, 2025, doi: 10.3390/met15020100.
-

- [30] R. D. B. Bobadilla, M. Baricco, and M. Palumbo, "Machine learning-driven prediction of glass-forming ability in Fe-based bulk metallic glasses using thermophysical features and data augmentation," *Metals*, vol. 15, no. 7, p. 763, 2025, doi: 10.3390/met15070763.
- [31] H. Balasooriya, C. Li, and F. Wang, "Understanding steel corrosion: Surface chemistry and defects explored through DFT modelling — A review," *Processes*, vol. 13, no. 7, p. 1971, 2025, doi: 10.3390/pr13071971.
- [32] Z. Li, W. Dai, H. Yue, C. Guo, Z. Ji, Q. Li, and J. Zhang, "Fatigue life prediction of 2024-T3 clad Al alloy based on an improved SWT equation and machine learning," *Materials*, vol. 18, no. 2, p. 332, 2025, doi: 10.3390/ma18020332.
- [33] A. Lehrfeld, K. Jaśkowiec, D. Wilk-Kołodziejczyk, M. Małysza, A. Bitka, Ł. Marcjan, and M. Głowacki, "Analysis of the possibility of making a digital twin for devices operating in foundries," *Electronics*, vol. 13, no. 2, p. 349, 2024, doi: 10.3390/electronics13020349.
- [34] U. M. Chaudry, K. Hamad, and T. Abuhmed, "Machine learning-aided design of aluminum alloys with high performance," *Materials Today Communications*, vol. 26, 2021, doi: 10.1016/j.mtcomm.2020.101897.
- [35] H. Fu, H. Zhang, C. Wang, W. Yong, and J. Xie, "Recent progress in the machine learning-assisted rational design of alloys," *International Journal of Minerals, Metallurgy and Materials*, vol. 29, no. 4, pp. 635–644, 2022, doi: 10.1007/s12613-022-2458-8.
- [36] I. Didych, O. Yasniy, I. Pasternak, and L. Sobashek, "Modelling of AL-6061 aluminum alloy deformation diagrams by machine learning methods," *Procedia Structural Integrity*, vol. 42, pp. 1344–1349, 2022, doi: 10.1016/j.mtcomm.2025.112420.
- [37] T. Beridze, Z. Baranik, I. Dashko, O. Hamova, and S. Tkachenko, "Fundamental imperatives of eliminating uncertainty on the basis of monitoring the activity of the iron ore enterprise," *Naukovyi Visnyk Natsionalnoho Hirnychoho Universytetu*, no. 3, pp. 151–157, 2023, doi: 10.33271/nvngu/2023-3/151.
- [38] J. L. Mullo, I. La Fé-Perdomo, J. Ramos-Grez, Á. F. Moreira Romero, A. Ramírez-Albán, M. Yarad-Jácome, and G. O. Barrionuevo, "Predicting the relative density of stainless steel and aluminum alloys manufactured by L-PBF using machine learning," *Journal of Manufacturing and Materials Processing*, vol. 9, no. 6, p. 185, 2025, doi: 10.3390/jmmp9060185.
- [39] L. Trykoz, S. Kamchatnaya, D. Borodin, A. Atynian, and R. Tkachenko, "Protection of railway infrastructure objects against electrical corrosion," *Anti-Corrosion Methods and Materials*, vol. 68, no. 5, pp. 380–384, 2021, doi: 10.1108/ACMM-05-2021-2483.
- [40] S. Zhao, Y. Shi, C. Huang, X. Li, Y. Lu, Y. Wu, Y. Li, and L. Wang, "Integrating machine learning into additive manufacturing of metallic biomaterials: A comprehensive review," *Journal of Functional Biomaterials*, vol. 16, no. 3, p. 77, 2025, doi: 10.3390/jfb16030077.
- [41] J. R. Davis (ed.), *Corrosion of Aluminum and Aluminum Alloys*, ASM International, 1999, ISBN 0-87170-629-6.
- [42] Y. Hryhoriev, S. Lutsenko, Y. Shvets, A. Kuttybayev, and N. Mukhamedyarova, "Predictive calculation of blasting quality as a tool for estimation of production cost and investment attractiveness of a mineral deposit development," *IOP Conference Series: Earth and Environmental Science*, vol. 1415, no. 1, p. 012027, 2024, doi: 10.1088/1755-1315/1415/1/012027.
- [43] A. Atynian, L. Trykoz, and D. Borodin, "Protection of railway infrastructure objects against electrical corrosion," *Baltic Journal of Road and Bridge Engineering*, 2021, Scopus-indexed, doi: 10.1108/ACMM-05-2021-2483.
- [44] V. Mytsa and M. Riabchykov, "Improvement of intelligent systems for creating personalized products," *CEUR Workshop Proceedings*, vol. 3896, pp. 235–247, 2024.
- [45] M. Pavlovskiy, "The improvement of fuel efficiency and environmental characteristics of diesel engine by using biodiesel fuels," in *Modern Technologies in Energy and Transport*, Springer, vol. 510, 2024, doi: 10.1007/978-3-031-44351-0_4.

-
- [46] A. Oralbekova, M. Amanova, K. Rustambekova, Z. Kaskatayev, O. Kisselyova, and R. Nurgaliyeva, "Conceptual model creation for automated self-training system of functional control and detection of railway transport," *International Journal of Electronics and Telecommunications*, vol. 67, no. 4, 2021.
- [47] S. Abdullayev, A. Izbairova, O. Khalilova, A. Tolesh, and I. Bondar, "Measurement of stresses in soils of road embankments with the help of Mesdoses," *International Journal of Innovative Research and Scientific Studies*, vol. 8, no. 2, pp. 1746–1754, 2025, doi: 10.53894/ijirss.v8i2.5539.
- [48] Y. Xiong, J. Robson, Z. Cao, Y. Deng, Y. Yao, X. Zhong, A. Bendo, J. Lv, F. Guarracino, J. Donoghue,
- [49] M. Curioni, and M. Curioni, "Mitigation effects of over-aging (T73) induced intergranular corrosion on stress corrosion cracking of AA7075 aluminum alloy and behaviors of η phase grain boundary precipitates during the intergranular corrosion formation," *Corrosion Science*, vol. 225, p. 111570, 2023, doi: 10.1016/j.corsci.2023.111570.
- [50] A. Kabdoldina, Z. Ualiyev, N. Smailov, F. Malikova, K. Oralkanova, M. Baktybayev, D. Arinova, A. Khikmetov, A. Shaikulova, and L. Bazarbay, "Development of the design and technology for manufacturing a combined fiber-optic sensor used for extreme operating conditions," *Eastern-European Journal of Enterprise Technologies*, vol. 5, no. 5-119, pp. 34–43, 2022, doi: 10.15587/1729-4061.2022.266359.
- [51] V. Simakhin, S. Bondar, H. Drieieva, O. Kovalenko, O. Drieiev, and M. Zhumadilova, "Multifractal properties of traffic generator based on Markov chains," in *CMiGIN*, pp. 567–579, 2019.
- [52] H. M. Hubal, "Mathematical description of the non-equilibrium state of symmetric particle systems," *International Journal of Applied Mathematics*, vol. 32, no. 5, pp. 767–774, 2019.
- [53] H. M. Hubal, "The Einstein law for the system 'Brownian particle in thermostat' based on the presented probability approach," *International Journal of Pure and Applied Mathematics*, vol. 93, no. 6, pp. 885–895, 2014.
- [54] V.-M. Cristea, M. Baigulbayeva, Y. Ongarbayev, N. Smailov, Y. Akkazin, and N. Ubaidulayeva, "Prediction of oil sorption capacity on carbonized mixtures of shungite using artificial neural networks," *Processes*, vol. 11, no. 2, p. 518, 2023, doi: 10.3390/pr11020518.